



Cite this: *RSC Appl. Polym.*, 2024, **2**, 1013

# Advancements in polymer nanoconfinement: tailoring material properties for advanced technological applications

Alberto Alvarez-Fernandez \*<sup>a</sup> and Jon Maiz \*<sup>a,b</sup>

The precise encapsulation of polymer chains within nanometer-scale spaces or structures has sparked a dynamic research field with vast potential for technological applications. Through confinement, properties such as morphology, thermal stability, and mechanical strength can be finely tuned, offering opportunities for advanced materials and biomedical devices. Various confinement methods, including nanoparticle encapsulation, planar thin films, and cylindrical confinement, induce unique alterations in polymer behaviour, affecting their optical, electronic, and thermal properties. The remarkable expansion in the applications of confined polymers across numerous research fields underscores the need for critical discussions on future potential. Therefore, this perspective article aims to identify key challenges and opportunities in this interdisciplinary research community, with a special focus on their practical applications.

Received 23rd July 2024,  
Accepted 30th October 2024

DOI: 10.1039/d4lp00234b

rsc.li/rscapppolym

## 1. Introduction

The precise encapsulation of polymer chains within nanometre-scale spaces or structures has emerged in recent decades as a dynamic and rapidly growing research field.<sup>1–3</sup> This growth is fuelled by its opportunities to tailor the properties of polymers for a wide range of technological applications, from the development of advanced materials to the fabrication of novel biomedical devices or sensors, among others.<sup>4</sup> Indeed, through confinement, properties such as polymer morphology, thermal stability, surface area, and mechanical properties can be easily tuned, especially when compared to their bulk counterparts.<sup>2,5–9</sup>

These alterations primarily arise from structural effects, such as the elongation of polymeric chains under the confinement regime. These structural changes lead to reduced chain entanglements and improved chain alignment, which in turn restrict the mobility of the polymeric chains. As a result, properties such as stiffness, strength, and toughness of the fabricated system are enhanced. Moreover, these changes also help prevent degradation processes, such as chain scission or cross-linking, which is essential for applications requiring high thermal stability, including microelectronics and aerospace industries.<sup>10–12</sup>

Additionally, the confinement of polymers into nanostructures can induce changes in their electronic structure and optical properties, leading to the development of novel materials for optoelectronic devices, photonics, and sensors.<sup>13</sup> Nanoconfinement can also lead to significant improvements in the surface area-to-volume ratio through the creation of different nanostructures such as pillars or fibers. This increase in surface area is beneficial for applications such as catalysis, sensing, and energy storage, where increased surface interactions can significantly improve performance by offering more active sites for chemical reactions, enhancing sensitivity to target analytes, or better efficiency in charge storage and transfer.<sup>14–16</sup>

Given these compelling reasons, it is unsurprising that significant research efforts have been dedicated to exploring and developing methodologies for successful and tailored polymer confinement. Based on the dimensionality of the host material, these methodologies are typically divided into three main categories: one-dimensional (1D),<sup>17</sup> two-dimensional (2D),<sup>18</sup> and three-dimensional (3D).<sup>11,19</sup>

In the case of 3D structures, polymer chains are adsorbed onto nanoparticle surfaces or encapsulated within their interior, especially in the case of porous or hollow nanoparticles, depending on the specific interaction between the polymer and the nanoparticle surface.<sup>11</sup> The presence of nanoparticles introduces a confining effect on the polymeric chains, significantly retarding processes such as crystal growth kinetics for semicrystalline polymers or enhancing the mechanical, optical, and electrical properties of the resulting

<sup>a</sup>Centro de Física de Materiales (CFM) (CSIC-UPV/EHU) – Materials Physics Center (MPC), Paseo Manuel de Lardizabal 5, 20018 Donostia-San Sebastián, Spain.  
E-mail: alberto.alvarez@ehu.eus, jon.maizs@ehu.eus

<sup>b</sup>IKERBASQUE-Basque Foundation for Science, Plaza Euskadi 5, 48009 Bilbao, Spain



nanocomposite. For instance, interactions between silica nanoparticles and polymer systems such as polystyrene (PS), poly(methyl methacrylate) (PMMA), or poly(ethylene oxide) (PEO) have demonstrated a significant impact on polymer thermal properties (by increasing their glass transition temperature ( $T_g$ )), crystallization dynamics (by slowing down crystallization kinetics), and the elasticity of the final composite (making it more rigid).<sup>11,20,21</sup>

Alternatively, both experimental and simulation studies have shown that the confinement of polymers into 1D structures results in deviations from their bulk properties.<sup>22,23</sup> A notable example of this phenomenon is the self-assembly of block copolymers (BCPs, a polymer system composed of two or more incompatible blocks covalently linked together).<sup>24</sup> Thus, thin film confinement can induce significant deviations from the predicted bulk phase-segregated structures.<sup>22</sup> For instance, Bai *et al.* demonstrated that by varying the film thickness of a bulk-gyroid forming polystyrene-*block*-polydimethylsiloxane (PS-*b*-PDMS) system, various thin film morphologies ranging from spheres, to cylinders, perforated lamellae, or gyroids, could be achieved.<sup>25</sup> Similarly, Knoll *et al.* further demonstrated the significance of film thickness on final morphology in thin films.<sup>26</sup> Thus, their investigation revealed a range of morphologies, including perforated lamellae or different orientations of cylindrical structures, as well as coexistence between distinct morphologies, all influenced by the degree of confinement.

Finally, under 2D confinement, polymer chains are constrained within narrow channels or cylindrical pores. This form of confinement typically occurs within meso- and microporous materials, such as mesoporous silica particles, KIT-6 based mesoporous materials, anodic aluminium oxide (AAO), anodic titanium oxide templates, patterned perfluoropolyether (PFPE) molds, or polydimethylsiloxane (PDMS) stamp templates.<sup>27–30</sup> In all cases, structural parameters such as pore size and aspect ratio play a crucial role in determining the properties of the confined polymers, leading to changes like reduced chain mobility, slower dynamics, and crystal orientation due to geometric confinement during crystallite growth. These factors also influence the transition from heterogeneous to homogeneous or surface nucleation, while increasing the overall crystallinity.<sup>5–7,9,31</sup>

Another advantage of cylindrical confinement, especially *via* AAO, is the possibility of removing the inorganic template, allowing the fabrication of well-ordered arrays of 1D polymeric nanostructures such as nanowires or nanopillars with entirely tuneable structural characteristics—including center-to-center distance, diameter, and height—based on the characteristics of the template used for their fabrication.<sup>18,31</sup> This allows not only the tuning of physical kinetics or crystallization behaviours, as previously mentioned but also other important characteristics such as the material's surface area. Alternative techniques such as electrospinning have also shown promising results in the objective of fabricating such polymeric structures with highly controllable surface-to-volume ratios. However, the nanofiber obtained usually presents a low degree of organiz-

ation, limiting its application in scenarios where high structural order is required.<sup>32</sup>

Therefore, this combination of the development of novel nanofabrication strategies, the study of associated physicochemical properties, and the achievement of tailored responses has triggered an incredible expansion in the application of confined polymers in many directions and at an unprecedented speed. This is demonstrated not only by the number of articles published per year focused on these materials—from 195 in 2000 to more than 790 in 2023 (Web of Science, “confinement” and “polymers”, May 2024)—but also by the number of research fields involved, spanning from material science and applied physics to optics, environmental science, engineering, and energy, among others. At this point, there is a clear necessity to engage in critical discussions not only about past developments but, more importantly, about the future potential of these materials. In response, this perspective article aims to identify key challenges and opportunities in this increasingly diverse and cross-disciplinary research community, focusing especially on practical applications.

## 2. Fabrication strategies: towards 3D confinement

As previously outlined, the main polymer confinement strategies are divided into three main families: nanoparticle (3D), cylindrical (2D), and thin film (1D) confinement methods. It is important to note that this work does not aim to offer a comprehensive overview of all available fabrication techniques. For in-depth exploration, readers are encouraged to refer to excellent reviews dedicated to the various fabrication methodologies.<sup>33–37</sup> Alternatively, we will describe here some of the state-of-the-art fabrication methodologies, introducing their importance in present and future research. While important research has been conducted into 1D and 2D confinement,<sup>17,31,38–40</sup> 3D confinement remains a challenge. Among the available fabrication methodologies, three stand out as the most promising for addressing this challenge: evaporation-induced confinement assembly (EICA), 3D AAO, and electrospinning (Fig. 1).

### 2.1. Evaporation-induced confinement assembly

While standard polymer emulsification has been widely used in polymer confinement,<sup>41</sup> more recently, researchers have gone one step further and studied the self-assembly of—especially BCPs—under the 3D confinement regime, developing the so-called EICA fabrication methodology.<sup>42–44</sup> This strategy relies on the formation of micro-nano-particles (0.5–100  $\mu\text{m}$  diameter) *via* established emulsification processes, such as stirring, vortex mixing, or ultrasounds, prior to their slow drying into solid microparticles. During this evaporation process, microphase segregation of the incompatible BCPs takes place, resulting in the formation of a well-defined internal nanostructure within the microparticle (Fig. 2A(i–iii)).<sup>45</sup>





**Fig. 1** Schematic framework of this perspective: from the fabrication of confined polymers to their properties and applications.

Following pioneering computational and simulation studies,<sup>19,46,47</sup> Lu and co-workers presented the first experimental example of microparticles with controllable internal nanostructure created following this methodology.<sup>48</sup> Since then, extensive research has been focused on the study of the different parameters governing BCP microphase segregation within the microparticle such as BCP molecular weight,<sup>49</sup> surfactant nature,<sup>50</sup> or organic solvent employed during the emulsification process.<sup>51</sup> While the internal structure of the microparticles can be tuned by adjusting the weight fraction of each block in the BCP (Fig. 2A(vii–ix)), researchers have also demonstrated that the overall shape of the nanoparticles can be controlled by varying the surfactant to BCP ratio used during the emulsification process, or by the addition of NPs to the system, such as CuPt nanorods,<sup>52</sup> polymeric NPs,<sup>53</sup> Fe<sub>2</sub>O<sub>3</sub> NPs,<sup>54</sup> or quantum dots.<sup>55</sup> These modifications enable the formation of microparticles with controllable external shapes such as ellipsoids or rods (Fig. 2A(v and vi)).

However, despite intensive research, there are still some challenges that need to be addressed. The first is related to the size distributions of the microparticles obtained; thus, the introduction of microfluidic-based fabrication technologies should increase the homogeneity of the particles. The second challenge is focused on the possibility of obtaining ordered monolayers using these confined objects as building blocks. Typical colloidal deposition techniques, such as dip-coating or Langmuir–Blodgett, should be explored in this research endeavour.

## 2.2. Three-dimensional anodic aluminium templates

As already introduced, AAO is a well-known inorganic porous oxide produced through the electrochemical oxidation of aluminium. This material is distinguished by its highly ordered, uniform nanoporous structure, which can be precisely controlled in terms of pore size, interpore distance, and overall thickness through variations in anodization parameters. This well-known chemistry and structural versatility make AAO one

of the most important methodologies for polymer 2D confinement. Through approaches such as melt infiltration, solution infiltration, and electrophoretic deposition, a wide variety of polymers have been confined within the AAO template, and the impact on their physicochemical properties has been precisely determined.<sup>66,67</sup>

However, more recently, novel methodologies in AAO fabrication have led to the development of more advanced nanopore arrays, enabling the fabrication of fully 3D architectures by generating interconnections between the vertical pores. These methodologies often include a two-step anodization procedure (normally defined as mild and hard anodization, respectively) to create the transversal nanochannels perpendicular to the vertical nanopores (Fig. 2B).<sup>68</sup> On the contrary, more recent approaches are based on the application of alternating current density profiles.<sup>57</sup> This methodology enables the fabrication of 3D AAO templates in a single step without any additional post-processing requirements, which reduces fabrication time and minimizes waste generation. These advantages enhance the applicability of these structures for polymer confinement, as will be further discussed in Section 3.

## 2.3. Electrospinning

Electrospinning is a versatile and straightforward technique enabling the fabrication of fibers with high surface area-to-volume ratios, ranging in diameter from a few micrometres to tens of nanometres. This technique has facilitated research into the mechanical and crystallization kinetics of polymers under confinement.<sup>69–71</sup> During electrospinning, a high voltage is applied to a polymer solution or melt, generating a charged jet that is attracted towards a grounded collector. As the jet moves towards the collector, solvent evaporation and stretching processes take place, resulting in the formation of ultrafine polymer fibers.<sup>72</sup> Through continuous research and refinement of these fundamental principles, and by manipulating conventional electrospinning apparatus, researchers have successfully achieved unique morphologies and structures (Fig. 2C(ii–vi)),<sup>32,73</sup> with techniques such as multi-axial electrospinning (Fig. 2C(i)),<sup>74,75</sup> centrifugal electrospinning (Fig. 2C(vii)),<sup>64,76,77</sup> or 3D electrospinning.<sup>78,79</sup> This increase in structural complexity also allows for the introduction of various functionalities or compositions into the fibers, enabling the development of materials with tailored properties.<sup>80</sup> Additionally, the confinement of polymers during fiber spinning is a complex process that enhances molecular orientation and crystallinity, thereby improving the mechanical and thermal properties of the resulting fibers. Understanding these effects is crucial for tailoring fiber properties for specific applications. Another significant innovation in electrospinning-based confined polymer fabrication is the development of needleless approaches. Advanced setups such as roller,<sup>81</sup> bubble,<sup>82</sup> and corona electrospinning have been successfully employed to scale up the production of confined polymeric fibres (Fig. 2(viii)).<sup>83</sup> These advancements have significantly expanded the applications of confined poly-





**Fig. 2** (A) General concept of microparticle formation from emulsions (i–iii). Confinement morphologies of PS-*b*-PB BCPs. Lamellar morphology in concentric (iv), intermediate (v), and axial arrangement (vi), depending on surfactant mixture. Cylindrical morphology (vii and viii). Closed packed spheres (ix). Adapted with permission.<sup>44</sup> Copyright 2020, Elsevier. Adapted with permission.<sup>56</sup> Copyright 2008, John Wiley & Sons Inc. (B) Schematic of a single-step fabrication approach for 3D AAO based on direct pulse application (i). FE-SEM images of 3D AAOs fabricated using a left square wave and centre sinusoidal wave (ii). P(VDF-TrFE) fibres obtained after polymer infiltration into single-step 3D AAO templates (iii). Adapted with permission.<sup>57</sup> Copyright 2024, Elsevier. Adapted with permission.<sup>58</sup> Copyright 2022, The Royal Society of Chemistry. (C) Schematic (i) and SEM images illustrating the diversity of electrospun fibre morphologies obtained following different casting methods (ii–vi). Adapted with permission.<sup>59</sup> Copyright 2004, American Chemical Society. Adapted with permission.<sup>60</sup> Copyright 2007, American Chemical Society. Adapted with permission.<sup>61</sup> Copyright 2012, American Chemical Society. Adapted with permission.<sup>62</sup> Copyright 2017, American Chemical Society. Adapted with permission.<sup>63</sup> Copyright 2020, Springer Nature. Schematic of a centrifugal electrospinning (CES) setup (vii). Adapted with permission.<sup>64</sup> Copyright 2018, Springer Nature. High-speed camera depicting jet formation (viii). Adapted with permission.<sup>65</sup> Copyright 2012 American Chemical Society.

meric fibers and facilitated the study of their mechanical, electronic, and optical properties. However, challenges remain, such as the incompatibility of the methods presented here with very low molecular weight polymers. This limitation arises from the low number of chain entanglements in such polymers, which restricts stable fiber formation.

### 3. Applications: bringing the lab to the fab

As previously mentioned, confined polymers play a crucial role in the development of advanced nanomaterials, enabling



numerous applications in materials science, engineering, bio-medicine, electronics, optics, and more. In this section, we will highlight some of the latest applications of these materials, with a focus on those with significant potential for industrial translation.

### 3.1. Optical applications

**3.1.1. Optical metamaterials.** Optical metamaterials, distinguished by their engineered subwavelength structures, provide unprecedented control over light propagation and interaction. When combined with confined polymers, they form an appealing platform for exploring novel optical phenomena and developing advanced optical devices. For instance, BCPs under 1D confinement have shown promising applications in fabricating high and tuneable refractive index surfaces,<sup>84,85</sup> antireflective coatings,<sup>86–88</sup> or negative refractive

index materials (Fig. 3A).<sup>89</sup> In this context, the precise control over the self-assembly process of BCPs enabled by 1D confinement in thin films allows for the creation of a comprehensive library of various morphologies. Thus, the 1D spatial confinement, combined with the strong segregation behaviour of incompatible BCPs, forces the polymer chains into highly ordered structures. This alternation of domains with different refractive index materials allows for fine-tune of optical properties, including refractive indices and reflectivity.<sup>90,91</sup> In this context, recent advancements such as the synthesis of more complex polymer chain architectures and sophisticated fabrication methods like iterative self-assembly, coupled with their confinement in 1D thin films, have unlocked new possibilities for achieving intricate structures such as hexagonally ordered nanorings,<sup>92</sup> hexagonal 2D Archimedean tiling patterns,<sup>96</sup> and ordered multicomponent nanoclusters,<sup>97</sup> difficult to obtain by

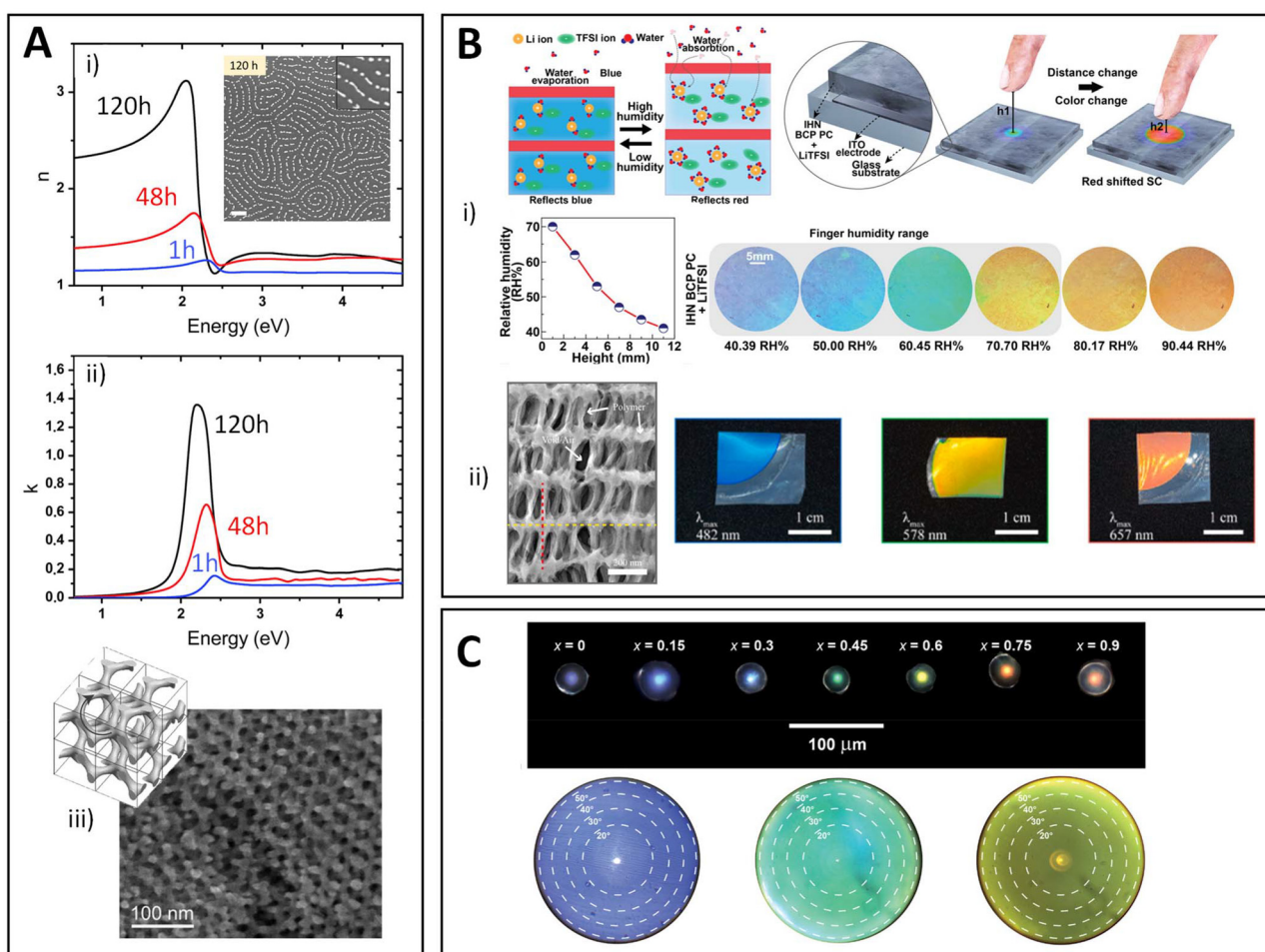


**Fig. 3** (A) Examples of high refractive index surfaces (i and ii) and 3D optical metamaterial (iii) created by BCP self-assembly. Adapted with permission.<sup>85</sup> Copyright 2018, The Royal Society of Chemistry. Adapted with permission.<sup>89</sup> Copyright 2011, John Wiley & Sons Inc. (B) Touchless sensing display produced via 1D BCP confinement (i) and STEM micrographs of the PE networks produced after the removal of the AAO template (left), alongside an optical image (right) demonstrating the structural coloration of the polymeric structures, which varies depending on the period of the AAO template employed (ii). Adapted with permission.<sup>93</sup> Copyright 2020 the Authors. Adapted with permission.<sup>94</sup> Copyright 2020 Elsevier Ltd. (C) Examples of photonic pigments based on BCP microparticles created via 3D EISA confinement. Shift in colour is related to changes in the internal structure of the microparticle. Adapted with permission.<sup>95</sup> Copyright 2022 John Wiley & Sons Inc.



other techniques. Finally, from an industrial perspective, new developments in the fabrication of confined thin films such as zone annealing, gradient thermal annealing, or the use of greener solvents have promoted their adoption for large-scale applications.<sup>98–101</sup>

**3.1.2. Bragg reflectors.** The concept of 1D polymer confinement, introduced earlier for its potential to control BCP self-assembly and create highly ordered materials, has been widely employed in fabricating Bragg reflectors (1D photonic crystals).<sup>102,103</sup> These structures typically involve alternating layers of materials to achieve the desired periodic variation in refractive index. This periodicity, with high and low refractive index domains, influences light propagation through the material, allowing or blocking specific wavelengths and thereby imparting a distinct structural colour. The 1D confinement of various polymer chain topologies, such as bottle brushes or BCPs, has facilitated the creation of surfaces with adjustable structural colours.<sup>104–107</sup> These characteristics have promoted their application in high-end technologies such as chemical,<sup>108,109</sup> mechanical,<sup>110,111</sup> or bio-sensors,<sup>112</sup> and also in the development of printable or touchless displays (Fig. 3B (i)).<sup>93,113</sup>

Beyond BCPs, the confinement of conventional polymers into more sophisticated structures, such as the 3D AAO structures discussed in Section 2.2, has also been explored in the fabrication of 1D photonic crystals. For instance, Martin and colleagues presented a straightforward, low-cost, and industrially scalable method to fabricate 3D polystyrene (PS) nanowires by replicating a 3D AAO template.<sup>68</sup> Interestingly, these nanostructures exhibit an intense green colour, contrasting with the colourless nature of standard PS films, underscoring the significant influence of confinement on the optical properties of the final material. Another notable example is the work of Resende *et al.*, where 3D AAO structures infiltrated with polyethylene (PE) materials of varying densities were utilized to create polymeric Bragg reflectors with tunable photonic responses (Fig. 3B(ii)).<sup>94</sup>

**3.1.3. Photonic pigments.** Advanced confinement strategies, such as the EICA method discussed in Section 2.1, have played a pivotal role in broadening the scope of polymeric systems for the production of photonic pigments. These pigments are based in the formation of microparticles with ordered internal structure, using normally amphiphilic BCPs and the previous introduces EICA fabrication methodology.<sup>95,116,117</sup> The 3D confinement effect within the microparticles, combined with BCP micro-segregation, leads to the formation of internal structures such as periodic concentric lamellar or onion-like nanostructures with alternating refractive indices. This allows the formation of structures with characteristics structural colours, based on the interspace of the created ordered structures. These materials have been proven essential for advancing paints, cosmetics, and displays, providing vibrant and pure colours that resist chemical and photo-bleaching—unlike many conventional pigments currently in use (Fig. 3C).<sup>114,115</sup>

## 3.2. Electronic applications

**3.2.1. Ferroelectricity.** Polar crystalline polymers can be categorized into four types: (i) normal ferroelectric polymers, which exhibit large hysteresis loops due to the switching of high spontaneous polarization. (ii) Paraelectric polymers, which can be polarized under an electric field but return to zero polarization once the field is removed. These polymers contain polar groups but maintain a non-polar crystalline phase. (iii) Relaxor ferroelectric polymers, which belong to a class of disordered crystals with compositional nanodomains. (iv) Antiferroelectric polymers, which belong to a class of ordered structures composed of two sublattices polarized spontaneously in antiparallel directions. These polymers can be polarized into a ferroelectric phase upon applying an electric field. The last two groups represent a novel category and are desirable for applications requiring high energy density and low-loss dielectrics.<sup>118</sup> Notable examples of ferroelectric crystalline polymers found in the literature include poly(vinylidene fluoride) (PVDF) and its copolymers, odd numbered nylons, cyanopolymers, polyurea/polythiourea, and biopolymers such as keratin and silk fibroin.<sup>119</sup>

Despite inhibited crystallization, different structural and performance properties can be enhanced under confinement conditions: (i) although crystallinity may be reduced, nanoconfinement typically induces preferential orientation of polymer chains in one direction. (ii) nanoconfinement often promotes the ferroelectric crystalline phase in both homopolymers and copolymers. (iii) the piezoelectric and ferroelectric responses, leading to improved active layer performance, are usually enhanced due to the increased polymorphic polar phases and crystal orientation.<sup>123</sup> For instance, Oh *et al.* successfully fabricated vertically well-aligned poly(vinylidene fluoride-trifluoroethylene) [P(VDF-TrFE)] nanorod arrays to enhance their ferroelectric properties, as illustrated in Fig. 4A.<sup>120</sup>

The primary application of ferroelectric polymers is in the fabrication of piezoelectric sensors.<sup>124</sup> For instance, Lan and colleagues recently introduced an acoustic piezoelectric sensor.<sup>125</sup> By using electrospinning to nanoconfine PVDF into 1D fibers, they achieved a 300% increase in the device's piezoelectric performance compared to its bulk counterpart. Another example involves ultrathin piezoelectric layers used to detect arterial pulse waves.<sup>126</sup> In this case, the 1D confinement into thin layers of the active material increased performance by a factor of 50. Other applications of nanoconfined ferroelectric polymers includes for example flexible self-charging batteries,<sup>127</sup> or even solar-steam generators, by the integration of ferroelectric fibers into highly hydratable light-absorbing poly(vinyl alcohol) (PVA) hydrogels.<sup>128</sup>

**3.2.2. Organic semiconductors.** The molecular design and chemical structure engineering of conjugated polymers, along with fabrication processes such as solution shearing, nanoconfinement, and electrospinning, significantly affect the final properties of these systems. In recent years, it has been observed that processing approaches, thickness, and nanoconfinement induce changes in physical properties due to inter-





**Fig. 4** (A) Example of ferroelectric P(VDF-TrFE) polymer nanostructure fabrication (i) and SEM images of the nanorod arrays (ii, iii). Adapted with permission.<sup>120</sup> Copyright 2012, Wiley-VCH GmbH. (B) Schematic illustration of the structural morphologies of semiconducting and insulating polymer blends films (i) and Arrhenius plot of the temperature-dependent linear hole mobility of a pure semiconducting polymer and blend OFET (ii). Adapted with permission.<sup>121</sup> Copyright 2021, Wiley-VCH GmbH. (C) Schematic of the nanowire fabrication process (i), photographs of the fabricated nanowire-filled AAO template (ii), with an inset showing a size comparison to a British one-pence coin, and SEM images of nanowires after template removal and a single Nylon nanowire strand (iii and iv), respectively. Adapted with permission.<sup>122</sup> Copyright 2017, The Royal Society of Chemistry.

facial and finite-size effects. Specifically, nanoconfinement plays a critical role in charge transport within conjugated polymer films. Park *et al.* have directly observed the effects of confinement on semiconducting polymers, especially within polymer blends, as demonstrated in Fig. 4B.<sup>121</sup> They systematically investigated the confinement effect based on the type of intermolecular interactions of semiconducting polymers within PS insulating matrices. Through this, they developed synergistic polymer blend systems that demonstrated a 3–4-fold improvement in field-effect hole mobilities, along with excellent optical transmittance exceeding 95% in the visible range. Polymer blending and BCP systems, influenced by nanoconfinement effects, can reduce the tensile modulus, increase stretchability, and raise the  $T_g$  without affecting carrier mobility. These parameters can enhance crystalline ordering, which is highly desirable for organic electronics applications.<sup>129,130</sup> Due to the unpredictable morphologies of conjugated thin films, 1D electrospun nanofibers or nanowires of conjugated polymers have proven to be a favourable tool for enhancing charge transport and crystallinity while reducing the bandgap compared to their bulk counterparts. This

approach offers the opportunity to reduce the size of devices while maintaining or even increasing their performance, stability, and mechanical properties.<sup>131</sup> Shin *et al.* demonstrate that semiconducting polymers, such as poly(3-hexylthiophene) (P3HT), can be confined into fibers through electrospinning techniques, offering high mechanical stability to transistors.<sup>132</sup> These advancements have significant implications for energy applications. For example, several research groups have recently investigated confining semiconducting polymers within AAO to form nanostructures in the active layers of organic solar cells, aiming to enhance their efficiency.<sup>133–135</sup>

**3.2.3. Triboelectric nanogenerators.** The ease of fabrication, innovative device design, diverse material availability, and exceptional power conversion efficiencies make triboelectric nanogenerators (TENGs) highly attractive for addressing the escalating challenges in the energy sector. TENGs have emerged as a powerful technology for harvesting mechanical energy through the coupling of triboelectrification and electrostatic induction. They offer unique advantages such as high power density, high efficiency, low weight, and low fabrication cost. One advantage of using nanoconfinement systems as



TENG active layers is the self-polarization of the nanowires. For example, when a polymer is confined within AAO templates, the nanoconfinement effect induces a preferential crystal orientation, increasing the average crystallinity of the material. This enhancement in crystallinity leads to highly efficient piezoelectric nanogenerators. Thus, Choi and co-workers demonstrated a 6-fold increase in the output power of triboelectric devices by confining Nylon-11 within AAO micropores, which led to a subsequent increase in crystallinity by up to 40% (Fig. 4C).<sup>122</sup> In addition, the formation of an electroactive-based electrospun system facilitates the development of the polar crystalline phase, enhancing dielectric properties. This results in superior performance and greater efficiency for the TENG.<sup>136</sup>

### 3.3. Thermal applications

**3.3.1. Phase change materials.** In recent years, the properties relevant to thermal energy storage, particularly those influenced by nanoconfinement, have gained significant attention due to the growing demand for efficient energy storage solutions in energy production. Phase change materials (PCMs) are especially important because they can store thermal energy as latent heat through phase transitions.

Thus, 2D confinement within polynorbornene-based bottle-brush polymer scaffolds has significantly enhanced the ability of paraffin to efficiently convert solar energy into latent heat storage.<sup>137</sup> Recently, Lu and co-workers have advanced the field by fabricating flexible and processable shape-stable polymer-based PCM films. They achieved this through a combination of electrospinning and hot-pressing technologies to induce confined crystallization, resulting in flexible PCMs that maintain their properties even at room temperature (Fig. 5A).<sup>138</sup>

AAO templates and porous silica matrices have also played an important role in the fabrication of polymer-based PCMs. Thus, Fang and co-workers have shown the important advances in heat storage properties of a series of thermoset-

ting polyurethanes (TPUs) by their confinement into AAO porous matrix.<sup>139</sup> Thus parameters such as fiber length and diameter (both determined by the AAO template) allowed for the tunability of heat energy storage properties of the material (Fig. 5B). Similar strategies using silica porous materials have also allowed for the obtention of polymer-based PCMs with controllable thermal properties.<sup>141,142</sup>

**3.3.2. Thermoelectric materials.** Energy recovery can be effectively achieved using thermoelectric materials, which facilitate the direct conversion between thermal and electrical energy. This process encompasses three distinct physical phenomena: the Seebeck effect, the Peltier effect, and the Thomson effect,<sup>143,144</sup> offering a viable solution for various technological applications. In the search for new thermoelectric materials, polymers have emerged as alternatives due to their lightweight nature, flexibility, and ease of processing compared to more conventional materials. However, improvements in their Seebeck coefficient and electrical conductivity are necessary before they can be utilized in large-scale devices.<sup>145</sup>

To address this, confining polymeric materials into 1D, 2D, and 3D structures has become a critical research area. This approach enhances the thermoelectric properties of polymers and advances their potential applications. Specifically, 1D thermoelectric materials have been recognized for their superior performance due to quantum confinement, which increases the density of states near the Fermi level and thus enhances the Seebeck coefficient.<sup>146–148</sup> This parameter is crucial for the performance of thermoelectric devices, often measured by the dimensionless figure of merit, ZT. Moreover, 1D materials exhibit effective phonon scattering due to a high density of interfaces, resulting in lower lattice thermal conductivity and higher ZT values.<sup>149,150</sup> Following the 1D confinement methodology, Wu and co-workers have recently developed highly efficient thermoelectric wearables (Fig. 5C).<sup>140</sup> This device is capable of harvesting energy from body heat and continuously



Fig. 5 (A) Schematic of the fabrication of polyether-based flexible PCMs. Adapted with permission.<sup>138</sup> Copyright 2024, American Chemical Society. (B) SEM illustrating the TPU nanoarrays obtained using different AAO nano-template diameters (i), and TPU melt points and enhanced coefficient of heat enthalpy as a function of nanoarray diameter (ii). Adapted with permission.<sup>139</sup> Copyright 2019, American Chemical Society (C) Schematic thermoelectric generator device (i) and its ability to activate an LED bulb (ii). Adapted with permission.<sup>140</sup> Copyright 2020, Elsevier.



self-powering, demonstrating the importance of advancing confinement technologies to enhance thermoelectric performance. In overall, confinement can enhance charge carrier mobility, reduce thermal conductivity, and leverage quantum effects to optimize thermoelectric properties. Success will be measured through improvements in the ZT, as well as practical performance metrics like durability and scalability.

**3.3.3. Thermal insulators.** The field of thermal insulation is gaining significant attention due to the increasing need to reduce energy waste in both industrial and domestic environments, the growing demand for home comfort, and the need for more efficient industrial processes.

Polymer nanocomposites represent highly effective materials for efficient energy use as thermal insulators. In general, amorphous polymeric materials diffuse heat slowly, making them ideal matrices for thermally insulating composites. Among various polymer systems, elastomers are particularly advantageous due to their additional functionality in providing vibroacoustic insulation. The final properties of these nanocomposites are largely determined by the fillers used. Interactions in the interfacial region (nanoconfinement effects) between the filler and the surrounding matrix play a crucial role in determining these properties.<sup>151</sup> Thus, Ma and co-workers have shown how polymer topology, allow for a complete tuning of PS thermal transport properties.<sup>152</sup> By adjusting the topology from linear to bottle-brush configurations, tailored thermal conductivities can be achieved, which is directly related to the distinct polymer chain motions in each system. Similarly, other researchers have highlighted confinement methods, such as 1D electrospun fibers or nanoparticle confinement, as crucial for fabricating low thermal conductivity polymers. These methods find applications in fire retardant materials and all-polymer insulating composites.<sup>153,154</sup>

## 4. Summary and perspective

The precise encapsulation of polymer chains within nanometer-scale spaces offers significant potential for tailoring polymer properties for a wide range of applications. The development of advanced nanofabrication strategies and the study of associated physicochemical properties have led to rapid advancements in the field.

One of the primary areas of research is the development of more advanced nanofabrication techniques. Current methods, while effective, often face challenges related to scalability, precision, and cost. Future advancements, like the ones presented here, are likely to focus on scalable fabrication techniques that allow for industrial production without sacrificing nanoscale precision. To this end, hybrid approaches combining existing nanofabrication methods such as 3D printing, nanoimprint lithography, or BCP self-assembly are expected to increase the complexity of the structures obtained through confinement.

Focusing on the applications, current environmental and energy challenges offer significant opportunities for polymer nanoconfinement. Consequently, there is growing interest in

polymer nanoconfinement for enhancing the efficiency of batteries, supercapacitors, and thermoelectric materials, contributing to the development of more efficient and sustainable energy systems. Furthermore, the development of flexible and lightweight confined polymer structures opens new avenues for wearable and portable energy devices.

Another important research field that is expected to gain importance in the coming years is the fabrication of multi-functional confined nanostructures. The confinement of smart polymeric materials that can respond to external stimuli, such as temperature, light, or pH, will enable the development of advanced materials with dynamic and adaptive properties. These responsive materials could lead to innovations in areas such as targeted drug delivery, self-healing materials, and adaptive coatings, while the confinement effect will allow for tuning their electronic, thermal, and mechanical properties.

Despite significant progress, fundamental research remains crucial for advancing the field of polymer nanoconfinement. Consequently, detailed studies on the molecular dynamics of polymer chains within confined spaces, particularly through theoretical simulations, have proven essential for developing predictive models that help reduce experimental efforts by identifying optimal conditions and structures needed to achieve desirable polymer properties.<sup>155,156</sup> This research endeavor is expected to continue and evolve. Thus, advancements in artificial intelligence (AI) and machine learning (ML) are expected to accelerate the design of new materials and confinement structures. Thus, by leveraging AI and ML it is possible to predict polymer microstructures based on processing conditions,<sup>157</sup> or even to design tailored polymer systems with optimal physical properties (*e.g.*, thermal, conductivity, mechanical).<sup>158</sup> These advancements have the potential to revolutionized the nanoconfinement research field, much like they are transforming another experimental area such as colloidal chemistry and nanoparticle synthesis.<sup>159</sup>

In conclusion, the future of polymer nanoconfinement is promising. Continued research and development will not only enhance the properties and functionalities of polymers but also pave the way for new technologies that address current challenges in fields such as nanomedicine, energy, and optics. Through these advancements, polymer nanoconfinement will continue to push the boundaries of material science, offering solutions to some of the most significant technological and societal challenges of our time.

## Data availability

No primary research results, software or code have been included and no new data were generated or analysed as part of this review.

## Conflicts of interest

There are no conflicts to declare.



## Acknowledgements

Grant No. PID2021-123438NB-I00 funded by MICIU/AEI/10.13039/501100011033 and ERDF/EU, Grant No. TED2021-130107A-I00 funded by MICIU/AEI/10.13039/501100011033 and “European Union NextGenerationEU/PRTR” are acknowledged. Additionally, financial support from Eusko Jaurlaritza (code: IT1566-22) and Gipuzkoako Foru Aldundia through the Programa de Red Guipuzcoana de Ciencia, Tecnología e Innovación (code: 2023-CIEN-000069-01) is acknowledged. A. A-F. is grateful for support from the Provincial Council of Gipuzkoa under the program Fellow Gipuzkoa.

## References

- L. M. Fonseca, E. P. D. Cruz, R. L. Crizel, C. Jansen-Alves, A. R. G. Dias and E. D. R. Zavareze, *Trends Food Sci. Technol.*, 2024, **147**, 104467.
- K. Chrissopoulou and S. H. Anastasiadis, *Soft Matter*, 2015, **11**, 3746–3766.
- C. B. Roth, *Chem. Soc. Rev.*, 2021, **50**, 8050–8066.
- E. Verde-Sesto, A. Arbe, A. J. Moreno, D. Cangialosi, A. Alegría, J. Colmenero and J. A. Pomposo, *Mater. Horiz.*, 2020, **7**, 2292–2313.
- J. Martín, M. Krutyeva, M. Monkenbusch, A. Arbe, J. Allgaier, A. Radulescu, P. Falus, J. Maiz, C. Mijangos, J. Colmenero and D. Richter, *Phys. Rev. Lett.*, 2010, **104**, 197801.
- M. Krutyeva, A. Wischniewski, M. Monkenbusch, L. Willner, J. Maiz, C. Mijangos, A. Arbe, J. Colmenero, A. Radulescu, O. Holderer, M. Ohl and D. Richter, *Phys. Rev. Lett.*, 2013, **110**, 108303.
- G. Liu, A. J. Müller and D. Wang, *Acc. Chem. Res.*, 2021, **54**, 3028–3038.
- R. M. Michell and A. J. Müller, *Prog. Polym. Sci.*, 2016, **54–55**, 183–213.
- M. Krutyeva, S. Pasini, M. Monkenbusch, J. Allgaier, J. Maiz, C. Mijangos, B. Hartmann-Azanza, M. Steinhart, N. Jalarvo and D. Richter, *J. Chem. Phys.*, 2017, **146**, 203306.
- P. Song, J. Dai, G. Chen, Y. Yu, Z. Fang, W. Lei, S. Fu, H. Wang and Z.-G. Chen, *ACS Nano*, 2018, **12**, 9266–9278.
- H. Wang, Y. Qiang, A. A. Shamsabadi, P. Mazumder, K. T. Turner, D. Lee and Z. Fakhraai, *ACS Macro Lett.*, 2019, **8**, 1413–1418.
- L. Liu, M. Zhu, X. Xu, X. Li, Z. Ma, Z. Jiang, A. Pich, H. Wang and P. Song, *Adv. Mater.*, 2021, **33**, 2105829.
- R. Periz, M. Geuß, N. Mameka, J. Markmann and M. Steinhart, *Small*, 2024, **20**, 2308478.
- V. Mouarrawis, R. Plessius, J. I. van der Vlugt and J. N. H. Reek, *Front. Chem.*, 2018, **6**, 419863.
- X. Li, B. Liu, J. Wang, S. Li, X. Zhen, J. Zhi, J. Zou, B. Li, Z. Shen, X. Zhang, S. Zhang and C.-W. Nan, *Nat. Commun.*, 2024, **15**, 6655.
- S. S. Kharintsev, E. A. Chernykh, A. V. Shelaev and S. G. Kazarian, *ACS Photonics*, 2021, **8**, 1477–1488.
- B. Frank, A. P. Gast, T. P. Russell, H. R. Brown and C. Hawker, *Macromolecules*, 1996, **29**, 6531–6534.
- J. Martín, J. Maiz, J. Sacristan and C. Mijangos, *Polymer*, 2012, **53**, 1149–1166.
- J. Fraaije and G. Sevink, *Macromolecules*, 2003, **36**, 7891–7893.
- J.-H. Wu, M. C. Kuo and C.-W. Chen, *J. Appl. Polym. Sci.*, 2015, **132**, 42378.
- X. Wen, Y. Su, G. Liu, S. Li, A. J. Müller, S. K. Kumar and D. Wang, *Macromolecules*, 2021, **54**, 1870–1880.
- W. Li, M. Liu, F. Qiu and A.-C. Shi, *J. Phys. Chem. B*, 2013, **117**, 5280–5288.
- T. Furuya and T. Koga, *Soft Matter*, 2018, **14**, 8293–8305.
- F. S. Bates, M. F. Schulz, A. K. Khandpur, S. Förster, J. H. Rosedale, K. Almdal and K. Mortensen, *Faraday Discuss.*, 1994, **98**, 7–18.
- W. Bai, A. F. Hannon, K. W. Gotrik, H. K. Choi, K. Aissou, G. Lontos, K. Ntetsikas, A. Alexander-Katz, A. Avgeropoulos and C. A. Ross, *Macromolecules*, 2014, **47**, 6000–6008.
- A. Knoll, A. Horvat, K. Lyakhova, G. Krausch, G. Sevink, A. Zvelindovsky and R. Magerle, *Phys. Rev. Lett.*, 2002, **89**, 035501.
- X.-H. Li, J.-C. Yu, N.-Y. Lu, W.-D. Zhang, Y.-Y. Weng and Z. Gu, *Chin. Phys. B*, 2015, **24**, 104215.
- L. Guo and M. Steinhart, *Appl. Surf. Sci.*, 2023, **639**, 158209.
- L. do Nascimento Batista, R. A. da Silva San Gil and M. I. Bruno Tavares, *Polym. Chem.*, 2024, **15**, 767–774.
- T. M. Díez-Rodríguez, E. Blázquez-Blázquez, R. Barranco-García, E. Pérez and M. L. Cerrada, *Macromol. Mater. Eng.*, 2022, **307**, 2200308.
- J. Maiz, J. Martín and C. Mijangos, *Langmuir*, 2012, **28**, 12296–12303.
- D. Li and Y. Xia, *Adv. Mater.*, 2004, **16**, 1151–1170.
- D. Richter and M. Kruteva, *Soft Matter*, 2019, **15**, 7316–7349.
- A. Romo-Urbe, *Polym. Adv. Technol.*, 2018, **29**, 507–516.
- Y.-X. Liu and E.-Q. Chen, *Coord. Chem. Rev.*, 2010, **254**, 1011–1037.
- S. Napolitano, E. Glynos and N. B. Tito, *Rep. Prog. Phys.*, 2017, **80**, 036602.
- J. M. Carr, D. S. Langhe, M. T. Ponting, A. Hiltner and E. Baer, *J. Mater. Res.*, 2012, **27**, 1326–1350.
- H. Wu, Y. Higaki and A. Takahara, *Prog. Polym. Sci.*, 2018, **77**, 95–117.
- Y. Li, D. Wei, C. C. Han and Q. Liao, *J. Chem. Phys.*, 2007, **126**, 204907.
- J. Kirk and P. Ilg, *Macromolecules*, 2017, **50**, 3703–3718.
- M. N. Vrancken and D. A. Claeys, Process for encapsulating water and compounds in aqueous phase by evaporation, *US. Pat.*, 3523906, 1970.
- I. Wyman, G. Njikang and G. Liu, *Prog. Polym. Sci.*, 2011, **36**, 1152–1183.



- 43 J. J. Shin, E. J. Kim, K. H. Ku, Y. J. Lee, C. J. Hawker and B. J. Kim, *ACS Macro Lett.*, 2020, **9**, 306–317.
- 44 C. K. Wong, X. Qiang, A. H. Müller and A. H. Gröschel, *Prog. Polym. Sci.*, 2020, **102**, 101211.
- 45 L. Li, K. Matsunaga, J. Zhu, T. Higuchi, H. Yabu, M. Shimomura, H. Jinnai, R. C. Hayward and T. P. Russell, *Macromolecules*, 2010, **43**, 7807–7812.
- 46 X. He, M. Song, H. Liang and C. Pan, *J. Chem. Phys.*, 2001, **114**, 10510–10513.
- 47 J. Feng, H. Liu and Y. Hu, *Fluid Phase Equilib.*, 2007, **261**, 50–57.
- 48 Z. Lu, G. Liu and F. Liu, *Macromolecules*, 2001, **34**, 8814–8817.
- 49 C. Chen, R. A. Wylie, D. Klinger and L. A. Connal, *Chem. Mater.*, 2017, **29**, 1918–1945.
- 50 D. Klinger, C. X. Wang, L. A. Connal, D. J. Audus, S. G. Jang, S. Kraemer, K. L. Killops, G. H. Fredrickson, E. J. Kramer and C. J. Hawker, *Angew. Chem.*, 2014, **126**, 7138–7142.
- 51 J. Zhu and R. C. Hayward, *J. Colloid Interface Sci.*, 2012, **365**, 275–279.
- 52 K. H. Ku, J. H. Ryu, J. Kim, H. Yun, C. Nam, J. M. Shin, Y. Kim, S. G. Jang, W. B. Lee and B. J. Kim, *Chem. Mater.*, 2018, **30**, 8669–8678.
- 53 M. Zhang, Z. Hou, H. Wang, L. Zhang, J. Xu and J. Zhu, *Langmuir*, 2020, **37**, 454–460.
- 54 Z. Hou, M. Ren, K. Wang, Y. Yang, J. Xu and J. Zhu, *Macromolecules*, 2019, **53**, 473–481.
- 55 H. Yang, K. H. Ku, J. M. Shin, J. Lee, C. H. Park, H.-H. Cho, S. G. Jang and B. J. Kim, *Chem. Mater.*, 2016, **28**, 830–837.
- 56 S. J. Jeon, G. R. Yi and S. M. Yang, *Adv. Mater.*, 2008, **20**, 4103–4108.
- 57 P. M. Resende, G. Hadziioannou and G. Fleury, *Mater. Today Commun.*, 2024, **39**, 109244.
- 58 C. V. Manzano, J. Rodríguez-Acevedo, O. Caballero-Calero and M. Martín-González, *J. Mater. Chem. C*, 2022, **10**, 1787–1797.
- 59 D. Li and Y. Xia, *Nano Lett.*, 2004, **4**, 933–938.
- 60 Y. Zhao, X. Cao and L. Jiang, *J. Am. Chem. Soc.*, 2007, **129**, 764–765.
- 61 W. Yuan and K.-Q. Zhang, *Langmuir*, 2012, **28**, 15418–15424.
- 62 T. Xu, H. Yang, D. Yang and Z.-Z. Yu, *ACS Appl. Mater. Interfaces*, 2017, **9**, 21094–21104.
- 63 A. Keirouz, N. Radacsi, Q. Ren, A. Dommann, G. Beldi, K. Maniura-Weber, R. M. Rossi and G. Fortunato, *J. Nanobiotechnol.*, 2020, **18**, 51.
- 64 L. Wang, B. Wang, Z. Ahmad, J.-S. Li and M.-W. Chang, *Drug Delivery Transl. Res.*, 2019, **9**, 204–214.
- 65 B. K. Brettmann, S. Tsang, K. M. Forward, G. C. Rutledge, A. S. Myerson and B. L. Trout, *Langmuir*, 2012, **28**, 9714–9721.
- 66 G. Liu, A. J. Muller and D. Wang, *Acc. Chem. Res.*, 2021, **54**, 3028–3038.
- 67 R. M. Michell, A. T. Lorenzo, A. J. Müller, M.-C. Lin, H.-L. Chen, I. Blaszczyk-Lezak, J. Martin and C. Mijangos, *Macromolecules*, 2012, **45**, 1517–1528.
- 68 J. Martín, M. Martín-González, J. Francisco Fernandez and O. Caballero-Calero, *Nat. Commun.*, 2014, **5**, 5130.
- 69 K. H. K. Chan, S. Y. Wong, X. Li, Y. Z. Zhang, P. C. Lim, C. T. Lim, M. Kotaki and C. B. He, *J. Phys. Chem. B*, 2009, **113**, 13179–13185.
- 70 W. A. Yee, M. Kotaki, Y. Liu and X. Lu, *Polymer*, 2007, **48**, 512–521.
- 71 M. V. Kakade, S. Givens, K. Gardner, K. H. Lee, D. B. Chase and J. F. Rabolt, *J. Am. Chem. Soc.*, 2007, **129**, 2777–2782.
- 72 S. Tripatanasuwan, Z. Zhong and D. H. Reneker, *Polymer*, 2007, **48**, 5742–5746.
- 73 A. Keirouz, Z. Wang, V. S. Reddy, Z. K. Nagy, P. Vass, M. Buzgo, S. Ramakrishna and N. Radacsi, *Adv. Mater. Technol.*, 2023, **8**, 2201723.
- 74 S. Kalantary, A. Jahani, R. Pourbabaki and Z. Beigzadeh, *RSC Adv.*, 2019, **9**, 24858–24874.
- 75 V. Kalra, J. H. Lee, J. H. Park, M. Marquez and Y. L. Joo, *Small*, 2009, **5**, 2323–2332.
- 76 F. Müller, S. Jokisch, H. Bargel and T. Scheibel, *ACS Appl. Polym. Mater.*, 2020, **2**, 4360–4367.
- 77 N. A. Norzain and W. C. Lin, *J. Ind. Text.*, 2022, **51**, 6728S–6752S.
- 78 M. Vong, F. J. D. Sanchez, A. Keirouz, W. Nuansing and N. Radacsi, *Mater. Des.*, 2021, **208**, 109916.
- 79 W. Feng, Y.-S. Zhang, Y.-W. Shao, T. Huang, N. Zhang, J.-H. Yang, X.-D. Qi and Y. Wang, *Eur. Polym. J.*, 2021, **145**, 110245.
- 80 D.-G. Yu, X.-Y. Li, X. Wang, J.-H. Yang, S. A. Bligh and G. R. Williams, *ACS Appl. Mater. Interfaces*, 2015, **7**, 18891–18897.
- 81 H. Niu, X. Wang and T. Lin, *J. Text. Inst.*, 2012, **103**, 787–794.
- 82 M. Ali, N. Anjum, Q. T. Ain and J.-H. He, *Fibers Polym.*, 2021, **22**, 1601–1606.
- 83 K. Molnar and Z. K. Nagy, *Eur. Polym. J.*, 2016, **74**, 279–286.
- 84 J. Y. Kim, H. Kim, B. H. Kim, T. Chang, J. Lim, H. M. Jin, J. H. Mun, Y. J. Choi, K. Chung and J. Shin, *Nat. Commun.*, 2016, **7**, 12911.
- 85 A. Alvarez-Fernandez, K. Aissou, G. Pécastaings, G. Hadziioannou, G. Fleury and V. Ponsinet, *Nanoscale Adv.*, 2019, **1**, 849–857.
- 86 H. Hulkkonen, A. Sah and T. Niemi, *ACS Appl. Mater. Interfaces*, 2018, **10**, 42941–42947.
- 87 C. Häggglund, G. Zeltzer, R. Ruiz, I. Thomann, H.-B.-R. Lee, M. L. Brongersma and S. F. Bent, *Nano Lett.*, 2013, **13**, 3352–3357.
- 88 P. Mokarian-Tabari, R. Senthamaraiannan, C. Glynn, T. W. Collins, C. Cummins, D. Nugent, C. O'dwyer and M. A. Morris, *Nano Lett.*, 2017, **17**, 2973–2978.
- 89 S. Vignolini, N. A. Yufa, P. S. Cunha, S. Guldin, I. Rushkin, M. Stefik, K. Hur, U. Wiesner, J. J. Baumberg and U. Steiner, *Adv. Mater.*, 2012, **24**, OP23–OP27.
- 90 A. Alvarez-Fernandez, C. Cummins, M. Saba, U. Steiner, G. Fleury, V. Ponsinet and S. Guldin, *Adv. Opt. Mater.*, 2021, **9**, 2100175.



- 91 L. Weihua, M. Liu and F. Qiu, *J. Phys. Chem. B*, 2013, **117**, 5280–5288.
- 92 A. Alvarez-Fernandez, F. Valdes-Vango, J. I. Martín, M. Vélez, C. Quirós, D. Hermida-Merino, G. Portale, J. M. Alameda and F. J. García Alonso, *Polym. Int.*, 2019, **68**, 1914–1920.
- 93 H. S. Kang, S. W. Han, C. Park, S. W. Lee, H. Eoh, J. Baek, D.-G. Shin, T. H. Park, J. Huh and H. Lee, *Sci. Adv.*, 2020, **6**, eabb5769.
- 94 P. M. Resende, E. Gutiérrez-Fernández, M. H. Aguirre, A. Nogales and M. Martín-González, *Polymer*, 2021, **212**, 123145.
- 95 A. Doderò, K. Djeghdi, V. Bauernfeind, M. Airoidi, B. D. Wilts, C. Weder, U. Steiner and I. Gunkel, *Small*, 2023, **19**, 2205438.
- 96 S. Antoine, K. Aissou, M. Mumtaz, G. Pécastaings, T. Buffeteau, G. Fleury and G. Hadziioannou, *Macromol. Rapid Commun.*, 2019, **40**, 1800860.
- 97 A. Alvarez-Fernandez, F. Nallet, P. Fontaine, C. Cummins, G. Hadziioannou, P. Barois, G. Fleury and V. Ponsinet, *RSC Adv.*, 2020, **10**, 41088–41097.
- 98 M. Luo and T. H. Epps III, *Macromolecules*, 2013, **46**, 7567–7579.
- 99 C. Cummins, A. Alvarez-Fernandez, A. Bentaleb, G. Hadziioannou, V. Ponsinet and G. Fleury, *Langmuir*, 2020, **36**, 13872–13880.
- 100 R. Lundy, S. P. Flynn, C. Cummins, S. M. Kelleher, M. N. Collins, E. Dalton, S. Daniels, M. A. Morris and R. Enright, *Phys. Chem. Chem. Phys.*, 2017, **19**, 2805–2815.
- 101 C. Cummins, R. Lundy, J. J. Walsh, V. Ponsinet, G. Fleury and M. A. Morris, *Nano Today*, 2020, **35**, 100936.
- 102 K. Zhu, C. Fang, M. Pu, J. Song, D. Wang and X. Zhou, *J. Mater. Sci. Technol.*, 2023, **141**, 78–99.
- 103 Z. Wang, C. L. C. Chan, T. H. Zhao, R. M. Parker and S. Vignolini, *Adv. Opt. Mater.*, 2021, **9**, 2100519.
- 104 B. R. Sveinbjörnsson, R. A. Weitekamp, G. M. Miyake, Y. Xia, H. A. Atwater and R. H. Grubbs, *Proc. Natl. Acad. Sci. U. S. A.*, 2012, **109**, 14332–14336.
- 105 C.-G. Chae, Y.-G. Yu, H.-B. Seo, M.-J. Kim, R. H. Grubbs and J.-S. Lee, *Macromolecules*, 2018, **51**, 3458–3466.
- 106 A. Noro, Y. Tomita, Y. Shinohara, Y. Sageshima, J. J. Walsh, Y. Matsushita and E. L. Thomas, *Macromolecules*, 2014, **47**, 4103–4109.
- 107 T. Guo, Y. Wang, Y. Qiao, X. Yuan, Y. Zhao and L. Ren, *Polymer*, 2020, **194**, 122389.
- 108 O. B. Ayyub, M. B. Ibrahim, R. M. Briber and P. Kofinas, *Biosens. Bioelectron.*, 2013, **46**, 124–129.
- 109 O. B. Ayyub, J. W. Sekowski, T.-I. Yang, X. Zhang, R. M. Briber and P. Kofinas, *Biosens. Bioelectron.*, 2011, **28**, 349–354.
- 110 E. P. Chan, J. J. Walsh, E. L. Thomas and C. M. Stafford, *Adv. Mater.*, 2011, **23**, 4702–4706.
- 111 T. H. Park, S. Yu, S. H. Cho, H. S. Kang, Y. Kim, M. J. Kim, H. Eoh, C. Park, B. Jeong and S. W. Lee, *NPG Asia Mater.*, 2018, **10**, 328–339.
- 112 Y. Fan, S. Tang, E. L. Thomas and B. D. Olsen, *ACS Nano*, 2014, **8**, 11467–11473.
- 113 H. S. Kang, J. Lee, S. M. Cho, T. H. Park, M. J. Kim, C. Park, S. W. Lee, K. L. Kim, D. Y. Ryu and J. Huh, *Adv. Mater.*, 2017, **29**, 1700084.
- 114 V. Hwang, A. B. Stephenson, S. Barkley, S. Brandt, M. Xiao, J. Aizenberg and V. N. Manoharan, *Proc. Natl. Acad. Sci. U. S. A.*, 2021, **118**, e2015551118.
- 115 Z. Li, X. Wang, L. Han, C. Zhu, H. Xin and Y. Yin, *Adv. Mater.*, 2022, **34**, 2107398.
- 116 Z. Cai, Z. Li, S. Ravaine, M. He, Y. Song, Y. Yin, H. Zheng, J. Teng and A. Zhang, *Chem. Soc. Rev.*, 2021, **50**, 5898–5951.
- 117 Y. Yang, H. Kim, J. Xu, M. S. Hwang, D. Tian, K. Wang, L. Zhang, Y. Liao, H. G. Park and G. R. Yi, *Adv. Mater.*, 2018, **30**, 1707344.
- 118 L. Zhu and Q. Wang, *Macromolecules*, 2012, **45**, 2937–2954.
- 119 H. S. Nalwa, *Ferroelectric polymers: chemistry: physics, and applications*, CRC Press, 1995.
- 120 S. Oh, Y. Kim, Y. Y. Choi, D. Kim, H. Choi and K. No, *Adv. Mater.*, 2012, **24**, 5708.
- 121 B. Park, H. Kang, Y. H. Ha, J. Kim, J. H. Lee, K. Yu, S. Kwon, S. Y. Jang, S. Kim and S. Jeong, *Adv. Sci.*, 2021, **8**, 2100332.
- 122 Y. S. Choi, Q. Jing, A. Datta, C. Boughey and S. Kar-Narayan, *Energy Environ. Sci.*, 2017, **10**, 2180–2189.
- 123 D. Guo, F. Zeng and B. Dkhil, *J. Nanosci. Nanotechnol.*, 2014, **14**, 2086–2100.
- 124 L. Zhang, S. Li, Z. Zhu, G. Rui, B. Du, D. Chen, Y.-F. Huang and L. Zhu, *Adv. Funct. Mater.*, 2023, **33**, 2301302.
- 125 B. Lan, X. Xiao, A. D. Carlo, W. Deng, T. Yang, L. Jin, G. Tian, Y. Ao, W. Yang and J. Chen, *Adv. Funct. Mater.*, 2022, **32**, 2207393.
- 126 M.-M. Laurila, M. Peltokangas, K. L. Montero, J. Verho, M. Haapala, N. Oksala, A. Vehkaoja and M. Mäntysalo, *Nano Energy*, 2022, **102**, 107625.
- 127 S. Yu, Y. Ling, S. Sun, Y. Wang, Z. Yu, J. Zheng, G. Liu, D. Chen, Y. Fu, Y. Liu and H. Zhou, *Nano Energy*, 2022, **94**, 106911.
- 128 S. Meng, C.-Y. Tang, J. Yang, M.-B. Yang and W. Yang, *Adv. Sci.*, 2022, **9**, 2204187.
- 129 H.-C. Tien, Y.-W. Huang, Y.-C. Chiu, Y.-H. Cheng, C.-C. Chueh and W.-Y. Lee, *J. Mater. Chem. C*, 2021, **9**, 2660–2684.
- 130 X. Wu, W. Fu and H. Chen, *ACS Appl. Polym. Mater.*, 2022, **4**, 4609–4623.
- 131 W. K. Tatum and C. K. Luscombe, *Polym. J.*, 2018, **50**, 659–669.
- 132 M. Shin, J. H. Song, G. H. Lim, B. Lim, J. J. Park and U. Jeong, *Adv. Mater.*, 2014, **22**, 3706–3711.
- 133 J. Ko, Y. Kim, J. S. Kang, R. Berger, H. Yoon and K. Char, *Adv. Mater.*, 2020, **32**, 1908087.
- 134 H. Park, H. Park, H. Ahn, W. Lee, J. Park, B. J. Kim and D. K. Yoon, *Chem. Mater.*, 2023, **35**, 1355–1362.



- 135 Y. Zhang, A. Chen, M.-W. Kim, A. Alaei and S. S. Lee, *Chem. Soc. Rev.*, 2021, **50**, 9375–9390.
- 136 S. Deswal, S. Arab, N. He, W. Gao, B. Lee and V. Misra, *RSC Appl. Polym.*, 2024, **2**, 634–641.
- 137 D. Fan, Y. Cao, J. Liu, D. Xiong and T. Qian, *Sol. Energy Mater. Sol. Cells*, 2022, **236**, 111547.
- 138 X. Lu, H. Huang, Y. Zhang, Z. Wang, C. Peng, S. Zhang, R. Lu, Y. Wang and B. Tang, *ACS Appl. Mater. Interfaces*, 2024, **16**, 38540–38549.
- 139 S. Fang, C. Li, L. Gao, Q. Sun, J. Cui, L. Zhou, C. Yang and H. Yu, *ACS Appl. Polym. Mater.*, 2019, **1**, 2924–2932.
- 140 K. Wu, Y. Zhang, F. Gong, D. Liu, C. Lei and Q. Fu, *Chem. Eng. J.*, 2021, **421**, 127764.
- 141 R.-A. Mitran, S. Ioniță, D. Lincu, D. Berger and C. Matei, *Molecules*, 2021, **26**, 241.
- 142 R.-A. Mitran, D. Berger and C. Matei, *Curr. Org. Chem.*, 2018, **22**, 2644–2663.
- 143 G. S. Nolas, J. Sharp and J. Goldsmid, *Thermoelectrics: basic principles and new materials developments*, Springer Science & Business Media, 2013.
- 144 C. Goupil, W. Seifert, K. Zabrocki, E. Müller and G. J. Snyder, *Entropy*, 2011, **13**, 1481–1517.
- 145 M. Goel and M. Thelakkat, *Macromolecules*, 2020, **53**, 3632–3642.
- 146 J. Ma, Q. Zhang, A. Mayo, Z. Ni, H. Yi, Y. Chen, R. Mu, L. M. Bellan and D. Li, *Nanoscale*, 2015, **7**, 16899–16908.
- 147 R. Shrestha, P. Li, B. Chatterjee, T. Zheng, X. Wu, Z. Liu, T. Luo, S. Choi, K. Hippalgaonkar and M. P. De Boer, *Nat. Commun.*, 2018, **9**, 1664.
- 148 X. Jiang, C. Ban, L. Li, J. Hao, N. Shi, W. Chen and P. Gao, *J. Appl. Polym. Sci.*, 2022, **139**, 52049.
- 149 R. Mohanraman, T.-W. Lan, T.-C. Hsiung, D. Amada, P.-C. Lee, M.-N. Ou and Y.-Y. Chen, *Front. Chem.*, 2015, **3**, 63.
- 150 R. Chen, J. Lee, W. Lee and D. Li, *Chem. Rev.*, 2019, **119**, 9260–9302.
- 151 A. Fraleoni-Morgera and M. Chhikara, *Adv. Eng. Mater.*, 2019, **21**, 1801162.
- 152 H. Ma and Z. Tian, *Appl. Phys. Lett.*, 2015, **107**, 073111.
- 153 G. Malucelli, F. Carosio, J. Alongi, A. Fina, A. Frache and G. Camino, *Mater. Sci. Eng., R*, 2014, **84**, 1–20.
- 154 X. Zhao, F. Yang, Z. Wang, P. Ma, W. Dong, H. Hou, W. Fan and T. Liu, *Composites, Part B*, 2020, **182**, 107624.
- 155 T. E. Gartner III and A. Jayaraman, *Macromolecules*, 2019, **52**, 755–786.
- 156 S. Maskey, J. M. D. Lane, D. Perahia and G. S. Grest, *Langmuir*, 2016, **32**, 2102–2109.
- 157 Z. Wan, S. Chen, X. Feng and Z.-Y. Sun, *Compos. Commun.*, 2024, **51**, 102072.
- 158 X. Huang, S. Ma, C. Y. Zhao, H. Wang and S. Ju, *npj Comput. Mater.*, 2023, **9**, 191.
- 159 H. Tao, T. Wu, M. Aldeghi, T. C. Wu, A. Aspuru-Guzik and E. Kumacheva, *Nat. Rev. Mater.*, 2021, **6**, 701–716.

